ENHANCED KNOWLEDGE IN SCIENCES AND TECHNOLOGY
e-ISSN: 2773-6385

EKST

Vol. 4 No. 1 (2024) 291-297
https://publisher.uthm.edu.my/periodicals/index.php/ekst

Influence of Sintering Temperature on Crystal Phase, Microstructure and Surface Resistivity: $Pr_{0.75}Na_{0.25}Mn_{0.98}Cr_{0.02}O_3$

Elly Shahira Mat Sidik[1], T. W. Lin[1], A. Azizi[1], Suhadir Shamsuddin[1]*

[1] *Ceramic and Amorphous Group, Department of Physics and Chemistry, Faculty of Applied Sciences and Technology, Universiti Tun Hussein Onn Malaysia Kampus Cawangan Pagoh, Hab Pendidikan Tinggi Pagoh, KM 1, Jalan Panchor, 84600 Pagoh, Muar, Johor, MALAYSIA.*

*Corresponding Author: suhadir@uthm.edu.my
DOI: https://doi.org/10.30880/ekst.2024.04.01.033

Article Info

Received: 27 December 2023
Accepted: 13 June 2024
Available online: 27 July 2024

Keywords

X-ray Diffraction, Scanning Electron Microscopy, Energy Dispersive X-ray Analysis, four-point probe

Abstract

Monovalent perovskite manganite of $Pr_{0.75}Na_{0.25}Mn_{0.98}Cr_{0.02}O_3$ has been investigated using different sintering temperatures (1100 °C, 1150 °C, and 1200 °C) on the crystal phase, microstructure, and surface resistivity. Despite the intriguing properties already demonstrated by manganite compounds, a comprehensive understanding of how sintering temperature influences monovalent perovskite manganites is still lacking. Employing a solid-state reaction method, samples underwent meticulous preparation and characterization using Powder X-ray Diffraction (XRD), Scanning Electron Microscopy (SEM) with Energy Dispersive X-ray Analysis (EDX), and a four-point probe for surface resistivity. XRD analysis reveals an orthorhombic structure with the *Pnma* group, demonstrating changes in lattice parameters from 225.1 $Å^3$ at 1100 °C, 225.6 $Å^3$ at 1150 °C to 225.8 $Å^3$ at 1200 °C. Other than that, the resistivity decreased from 117.1377Ω, 101.5461Ω, 97.0974Ω respectively. SEM imaging highlights irregular grain shapes, with heightened densification at higher temperatures. Furthermore, EDX measurements confirm the accurate composition of all samples, devoid of impurity peaks. The precise determination of the elemental composition percentages included Pr, Na, Mn, Cr, and O. Hence, different sintering temperatures affected the lattice parameter as well as the decreasing in microstructure and the resistivity.

1. Introduction

Monovalent perovskite manganite, with the general formula ABO_3 where A represents a monovalent cation typically derived from alkali metals, B signifies a trivalent manganese cation, and O serves as the oxygen anion, has attracted significant attention within the scientific community. This attention is due to its extraordinary properties, including colossal magnetoresistance (CMR) [1], the Jahn-Teller effect [2], and charge ordering (CO) [2-4]. Previous studies have demonstrated that monovalent-doped perovskite manganites exhibit distinct properties in terms of structural and surface morphology when subjected to monovalent metal doping [4]. For instance, previous study on $Pr_{0.75}Na_{0.25}MnO_3$ with Cr doped at Mn-site [4] have shown the Jahn-Teller (JT) effect which caused the charge ordered (CO) state to be weakened, and SEM images were quite uniform due to the good crystalline nature. While extensive research has delved into the properties of both divalent and monovalent doped manganites, this study uniquely focuses on the monovalent perovskite manganite compound $Pr_{0.75}Na_{0.25}Mn_{0.98}Cr_{0.02}O_3$. The selection of this specific compound is driven by the necessity for a more nuanced

exploration of monovalent perovskite manganites, which remains a relatively underexplored domain. The investigation of $Pr_{0.75}Na_{0.25}Mn_{0.98}Cr_{0.02}O_3$ allows us to fill a critical gap in the current understanding of the intricate interactions within this class of materials. Despite the wealth of studies varying the dopant concentration in parent compounds, a noticeable gap exists in our understanding—the influence of sintering temperature on perovskite manganites. This intentional choice aims to delve deeper into the nuanced interactions within this class of materials, specifically addressing the influence of sintering temperature on crystal phase, microstructure, and surface resistivity.

Acknowledging the pivotal role of sintering in shaping crystalline structure, density, and porosity [5], our investigation deliberately focuses on $Pr_{0.75}Na_{0.25}Mn_{0.98}Cr_{0.02}O_3$ —a monovalent perovskite manganite compound. However, existing research predominantly explores the impact of doping on these materials, this study diverges by specifically investigating the sintering effect on the monovalent perovskite manganite compound $Pr_{0.75}Na_{0.25}Mn_{0.98}Cr_{0.02}O_3$. The choice to focus on the sintering effect, as opposed to traditional doping studies, is driven by the understanding that sintering temperature plays a pivotal role in determining the final crystalline structure of the material [5]. The comparison of the sintering effects at varying temperatures will serve as a crucial aspect of this study. Through a meticulous analysis of the outcomes at 1000 °C, 1150 °C, and 1200 °C, a comparative evaluation will be conducted to discern the temperature-dependent variations in crystal phase, microstructure, chemical bonding, and surface resistivity. This comparative approach will provide a comprehensive understanding of the subtle nuances in material properties induced by different sintering conditions, offering valuable insights for future material optimization and application.

2. Materials and Methods

The synthesis of $Pr_{0.75}Na_{0.25}Mn_{0.98}Cr_{0.02}O_3$ manganite employed the solid-state reaction method, incorporating a series of processes. Investigation into the crystalline structure was conducted through X-ray Diffraction (XRD) analysis using a Bruker D2 Phaser Powder X-ray diffractometer model. Cu Kα radiation was employed to elucidate the composition of crystal phases. Microstructure and elemental compositions were analysed using a Coxem EM-30AX Plus model Scanning Electron Microscope (SEM) equipped with Energy Dispersive X-ray analysis (EDX). Electrical properties were scrutinized using a four-point probe setup, facilitating precise measurement of sheet resistance for a comprehensive understanding of the samples' electrical behaviour.

2.1 Chemical and Apparatus

The fabrication of manganite samples utilized high-purity Pr_2O_3, Na_2CO_3, MnO_2, Cr_2O_3 powders, each with a purity level of 99.99%. Advanced instruments employed in the study comprised the high-sensitivity digital electronic balance EJ-OP-13 Density Determination Kit, an agate mortar and pestle, an alumina crucible, the Protherm Furnace PLF 130/15 box furnace, the Bruker D2 Phaser model for powder X-ray diffraction, the Coxem EM-30AX Plus model for scanning electron microscopy, and a four-point probe setup for surface resistivity.

2.2 Sample Preparation

The synthesis of $Pr_{0.75}Na_{0.25}Mn_{0.98}Cr_{0.02}O_3$ manganite involved the solid-state reaction method. A precisely stoichiometric blend of Pr_2O_3, Na_2CO_3, MnO_2, and Cr_2O_3, each exhibiting purity levels exceeding 99.99%, underwent thorough mixing and grinding in an agate mortar with a pestle for approximately 2 hours. This meticulous process ensured a homogeneous mixture, resulting in a finely powdered substance. The composite powder underwent calcination at 1000 °C for 24 hours, gradually heated at a rate of 15 °C/min in a Protherm Furnace Model PLF130/15. Intermediate grinding intervals were interspersed with the calcination process, followed by controlled cooling at a rate of 1 °C/min. Subsequently, the powder underwent further refinement through grinding and was molded into pellets with dimensions of 13 mm in diameter and 2-3 mm in thickness using Specac Dice Mole. Compaction was achieved under a load of 5 tons utilizing a Carver Hydraulic Presser Equipment Model 3851. The resulting pellets were sintered at 1100 °C, 1150 °C, and 1200 °C for 24 hours in ambient air, heated at a rate of 15 °C/min, and gradually cooled to room temperature at 1 °C/min.

2.3 Sample Characterization

Various analytical methods were employed for the structural analysis of the specimens. X-ray Diffraction (XRD) examination, utilizing Cu Kα radiation at ambient temperature, was carried out using a Bruker D2 Phaser model powder XRD. The scanning parameters covered a 2θ range from 20° to 80° with a scanning rate of 2°/min, ensuring a meticulous evaluation of the crystalline structure and phase composition. SigmaPlot software was utilized for subsequent analysis of XRD patterns. For microstructure investigation, a Coxem EM-30AX Plus model Scanning Electron Microscope (SEM) was used at a magnification of 2kX. It is noteworthy that SEM

Enhanced Knowledge in Sciences and Technology Vol. 4 No. 1 (2024) p. 291-297

analysis employed pellet samples instead of powder, allowing for a thorough exploration of morphology and grain boundaries. This SEM analysis was complemented by energy dispersive X-ray spectroscopy (EDX) to determine the elemental composition of the specimens. To assess electrical properties, a four-point probe setup was employed for surface resistivity measurements. Additionally, bulk density was determined using the Archimedes principle, with acetone serving as the buoyant medium.

3. Results and Discussion

3.1 X-ray Diffraction (XRD)

Fig.1 depicts the X-ray Diffraction (XRD) patterns of $Pr_{0.75}Na_{0.25}Mn_{0.98}Cr_{0.02}O_3$ samples after sintering at temperatures of 1100°C, 1150°C, and 1200°C. The XRD analysis confirms the presence of an orthorhombic structure with the Pnma space group across all samples, indicating that the crystalline structure remains unaltered despite variations in sintering temperature, aligning with prior research [6-7]. No discernible impurity peaks or secondary peaks were identified. Table 1 offers a comprehensive summary of lattice parameters, unit cell volume (V), bulk density (bulk), and resistivity (Ω) for $Pr_{0.75}Na_{0.25}Mn_{0.98}Cr_{0.02}O_3$ following sintering at 1100°C, 1150°C, and 1200°C. The lattice parameters (a, b, and c) display subtle variations, with the a-lattice and c-lattice exhibiting an increase-decrease trend, while the b-lattice demonstrates a decrease-increase pattern as the sintering temperature progresses from 1100°C to 1200°C. The unit cell volume (V) demonstrates a decreasing trend, indicating structural modifications associated with Jahn–Teller distortion and alterations in Mn–O–Mn bond angles. Bulk density increases with higher sintering temperatures, suggesting a denser packing of grains. Elevated temperatures likely lead to better material compaction, reducing void spaces and increasing bulk density. The resistivity (Ω) values decrease with rising sintering temperature, indicating improved conductivity, possibly due to enhanced mobility of charge carriers at higher temperatures.

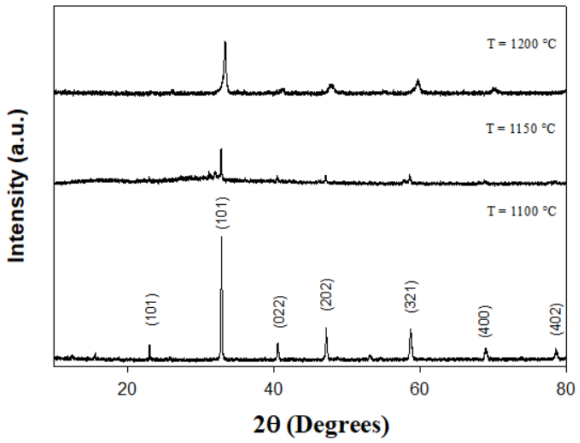

Fig. 1 *XRD analysis of $Pr_{0.75}Na_{0.25}Mn_{0.98}Cr_{0.02}O_3$ sintered at 1100 °C, 1150 °C, and 1200 °C*

Table 1 *Lattice Parameters, Unit Cell Volume (V), Bulk Density (ρ_{bulk}) and Resistivity (Ω) of $Pr_{0.75}Na_{0.25}Mn_{0.98}Cr_{0.02}O_3$ sintered at 1100 °C, 1150 °C, and 1200 °C*

Sintering temperature	Lattice parameter, Å (± 0.001)			V (Å^3)	ρbulk (g/cm^3)	Resistivity (Ω)
(°C)	a (Å)	b (Å)	c (Å)	(± 0.1)	(± 0.001)	(± 0.0001)
1100	5.473	7.878	5.220	225.1	4.302	117.1377
1150	5.474	7.890	5.224	225.6	6.871	101.5461
1200	5.475	7.893	5.226	225.8	7.101	97.0974

3.2 Scanning Electron Microscopy (SEM)

Fig. 2 depicts the microstructure of all samples, offering insights into the microstructural characteristics of $Pr_{0.75}Na_{0.25}Mn_{0.98}Cr_{0.02}O_3$ at different sintering temperatures. Utilizing SEM images captured at a 2kX magnification, a thorough examination of the material's microstructure was conducted. A discernible trend emerges with an increase in sintering temperature, revealing compact grain boundaries and a reduction in grain size growth. Elevated sintering temperatures tend to facilitate grain size growth and agglomeration, resulting in a more compact microstructure with closely packed grains [8-13]. At 1100°C, the samples display irregular shapes with minimal porosity, making grain boundaries barely visible. Progressing to 1150°C, an increase in average grain size suggests a densification process during sintering, contributing to a more compact microstructure. However, SEM imaging at the higher sintering temperature of 1200°C lacks clear and distinguishable microstructural features. The lack of clarity in these images may be attributed to various factors, including potential over-sintering leading to agglomeration, surface modifications, or other challenges specific to the conditions at this temperature.

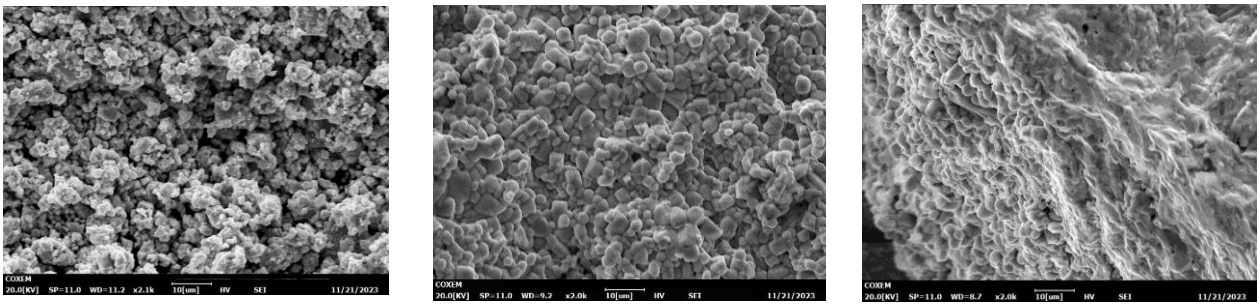

(a) **(b)** **(c)**

Fig. 2 *SEM imaging for the sample $Pr_{0.75}Na_{0.25}Mn_{0.98}Cr_{0.02}O_3$ sintered at (a) 1100 °C (b) 1150 °C and (c) 1200 °C with 2kX magnification*

Enhanced Knowledge in Sciences and Technology Vol. 4 No. 1 (2024) p. 291-297

3.3 Energy Dispersive X-ray Analysis (EDX)

Fig. 3 presents the spectrum of the EDX analysis for all the samples, specifically the $Pr_{0.75}Na_{0.25}Mn_{0.98}Cr_{0.02}O_3$ samples sintered at 1100 °C, 1150 °C, and 1200 °C. At the temperature of 1100 °C, the composition of $Pr_{0.75}Na_{0.25}Mn_{0.98}Cr_{0.02}O_3$ is highlighted, with dominant elements by weight percentage being praseodymium (Pr) (69.13%) and oxygen (O) (26.51%), constituting 21.50% and 76.23% of the atomic composition, respectively. Na, Mn, and Cr contribute smaller percentages, indicating their lesser presence in the material. As the temperature increases to 1150 °C, Pr remains the primary element by weight (61.46%), followed by Mn (16.37%) and O (20.12%). The atomic percentages reflect a similar hierarchy, emphasizing the prevalence of Pr and O in the atomic composition. At the temperature of 1200 °C, the elemental distribution is consistent with that at 1150 °C, reiterating the dominance of Pr and O, with Mn also playing a significant role.

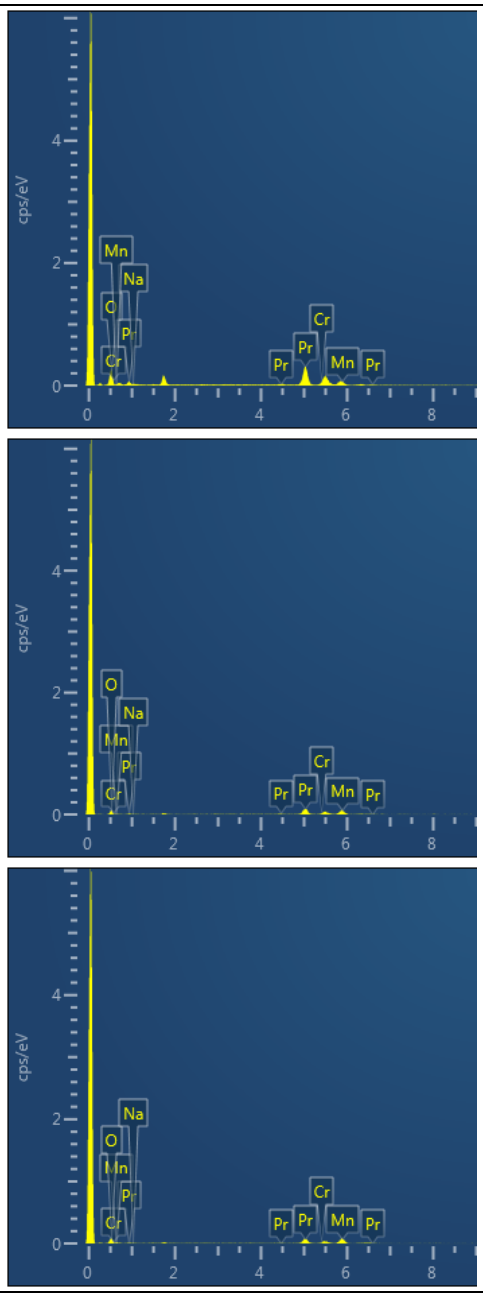

Element	Weight %	Atomic %
Pr	69.13	21.50
O	26.51	76.23
Na	2.11	4.02
Mn	1.18	0.94
Cr	1.08	0.91

Element	Weight %	Atomic %
Pr	61.46	21.36
Mn	16.37	14.59
O	20.12	61.56
Na	0.47	1.00
Cr	1.58	1.49

Element	Weight %	Atomic %
O	23.55	62.71
Pr	50.29	15.20
Mn	22.57	17.50
Na	1.59	2.94
Cr	2.01	1.64

Fig. 3 *EDX spectrum for the sample $Pr_{0.75}Na_{0.25}Mn_{0.98}Cr_{0.02}O_3$ with sintering temperatures of 1100 °C, 1150 °C, and 1200 °C*

4. Conclusion

In summary, the impact of varying sintering temperatures (1100 °C, 1150 °C, and 1200 °C) on $Pr_{0.75}Na_{0.25}Mn_{0.98}Cr_{0.02}O_3$ manganite has been studied. XRD analysis elucidated a consistent orthorhombic structure with the Pnma space group across all temperatures, underscoring the resilience of the crystal phase to sintering variations. Subtle variations in lattice parameters and unit cell volume suggested structural modifications. Densification increased with higher temperatures, as evidenced by rising bulk. Resistivity values decreased, indicating improved electrical conductivity. On the other hand, SEM revealed a trend of compacting grain boundaries and reduced grain size growth with elevated temperatures, but challenges in imaging clarity were noted at 1200 °C. EDX analysis highlighted the dominance of Pr and O across temperatures, emphasizing compositional stability.

Acknowledgement

The authors would like to thank the Material Physics Laboratory, Faculty of Applied Sciences and Technology, Pagoh Higher Education Hub, Universiti Tun Hussein Onn Malaysia, 84600 Panchor, Johor for the facilities provided

Conflict of Interest

Authors declare that there is no conflict of interests regarding the publication of the paper.

Author Contribution

The authors confirm contribution to the paper as follows: ***study conception and design, data collection, methodology, analysis and interpretation of results:*** *Elly Shahira Mat Sidik, T. W. Lin, A. Azizi and Suhadir Shamsuddin. All authors reviewed the results and approved the final version of the manuscript.*

References

[1] Razali, S. A., Ibrahim, N., Shamsuddin, S., & Noh, M. Z. (2018). Observation of charge ordering signal in monovalent doped $Nd_{0.75}Na_{0.25-x}KxMn_1O_3$ ($0 \leq x \leq 0.10$) manganates. *International Journal of Engineering and Technology*, *7*(4.3), 85-88.

[2] Shamsuddin, S., Ibrahim, N., Mayzan, M. Z. H., Esa, F., & Razali, S. A. (2022, June). Analysis of Electrical Transport Properties in $Nd_{0.75}Na_{0.25-x}K_xMnO_3$ Manganites. In *Proceedings of the 7th International Conference on the Applications of Science and Mathematics 2021: Sciemathic 2021* (pp. 139-145). Singapore: Springer Nature Singapore. https://link.springer.com/chapter/10.1007/978-981-16-8903-1_14

[3] Khairulzaman, N. N., Shamsuddin, S., & Ibrahim, N. (2020). Effect of Ag-doped on electrical transport properties in Pr0. 75Na0. 25MnO3 manganites. *Journal of Advanced Research in Dynamical and Control Systems*, *12*(2), 759-765. http://eprints.uthm.edu.my/id/eprint/6525

[4] Zawawi, R. A., Ibrahim, N., & Shamsuddin, S. (2018). Enhancment of double-exchange mechanism in charge-ordered Pr0. 75Na0. 25MnO3 ceramic by Cr doped at Mn-site. *International Journal Current Science, Engineering and Technology*, *1*(S1), 101-106.

[5] Teoh, W., & Suhadir Shamsuddin. (2022). Effect of Sintering Temperature on Structural and Surface Morphology of Manganite: Pr0.75Na0.25-xAgxMnO3. *Enhanced Knowledge in Sciences and Technology*, *2*(2), 052–059. Retrieved from https://penerbit.uthm.edu.my/periodicals/index.php/ekst/article/view/5443

[6] Khairulzaman, N., Ibrahim, N., & Shamsuddin, S. (2018). Impact of Ag-Doped on the Ferromagnetic-Metallic Transition in Pr0. 75Na0. 25mno3 Manganites. *International Journal of Engineering & Technology*, *7*(4.30), 68-71. http://www.sciencepubco.com/index.php/IJET

[7] Amaran, N. A., Ibrahim, N., & Mohamed, Z. (2023). Structural and Morphology Changes in PrMnO3 Manganite Induced by Ba (x= 0.33) Doping. *Journal of Advanced Research in Applied Sciences and Engineering Technology*, *29*(3), 160-167. https://doi.org/10.37934/araset.29.3.160167

[8] Shamsuddin, S., Ibrahim, A. B. M., & Yahya, A. K. (2013). Effect of Er substitution on ultrasonic anomaly in Dy0. 5− xErxBa0. 5CoO3 cobaltates. *Ultrasonics*, *53*(6), 1084-1088. https://doi.org/10.1016/j.ultras.2013.02.002

[9] Zawawi, R. A., Khairulzaman, N. N., & Shamsuddin, S. (2017). Effect of Cr-doped on Crystalline Phase, Surface Morphology and Electrical Properties of Charge-Ordered Nd0.75Na0.25MnO3 Ceramics. *Journal of Science and Technology*, *9*(3). Retrieved from https://publisher.uthm.edu.my/ojs/index.php/JST/article/view/2042

[10] Abdullah, T. D. N. (2022). Effect of Pectin Coating Enriched with Oregano Essential Oil on the Fresh-Cut Papaya Quality. *Enhanced Knowledge in Sciences and Technology*, *2*(1), 069-078.

[11] SATRIA, A. H. B. M. (2022). Isolation and characterization of biosurfactant-producing lactic acid bacteria from sauerkraut. *Enhanced Knowledge in Sciences and Technology*, *2*(2), 060-069.
[12] Liu, Y., Sun, T., Dong, G., Zhang, S., Chu, K., Pu, X., ... & Liu, X. (2019). Dependence on sintering temperature of structure, optical and magnetic properties of La0. 625Ca0. 315Sr0. 06MnO3 perovskite nanoparticles. *Ceramics International*, *45*(14), 17467-17475.
[13] Othman, S. A., & Fadzil, N. F. (2021). Utilization and valorization of Citrus Fruit by-products: A Review. *Enhanced Knowledge in Sciences and Technology*, *1*(2), 170-176.